SUPPLEMENTAL MATERIAL

SINGLE CELL RNA SEQUENCING REVEALS RENAL ENDOTHELIUM HETEROGENEITY AND (METABOLIC) ADAPTATION TO WATER DEPRIVATION

Sébastien J. Dumas[1-3], Elda Meta[1,3*], Mila Borri[1,3*], Jermaine Goveia[1,3], Katerina Rohlenova[1,3], Nadine V. Conchinha[1,3], Kim Falkenberg[1,3], Laure-Anne Teuwen[1,3], Laura de Rooij[1,3], Joanna Kalucka[1,3], Rongyuan Chen[2], Shawez Khan[1,3], Federico Taverna[1,3], Weisi Lu[2], Magdalena Parys[1,3], Carla De Legher[1,3], Stefan Vinckier[1,3], Tobias K. Karakach[1,3&], Luc Schoonjans[1-3], Lin Lin[4,5], Lars Bolund[4,5], Mieke Dewerchin[1,3], Guy Eelen[1,3], Ton J. Rabelink[6], Xuri Li[2#], Yonglun Luo[4,5,7,8#], Peter Carmeliet[1-3#]*

SUPPLEMENTAL MATERIAL: TABLE OF CONTENTS

Figure S1

A FACS strategy

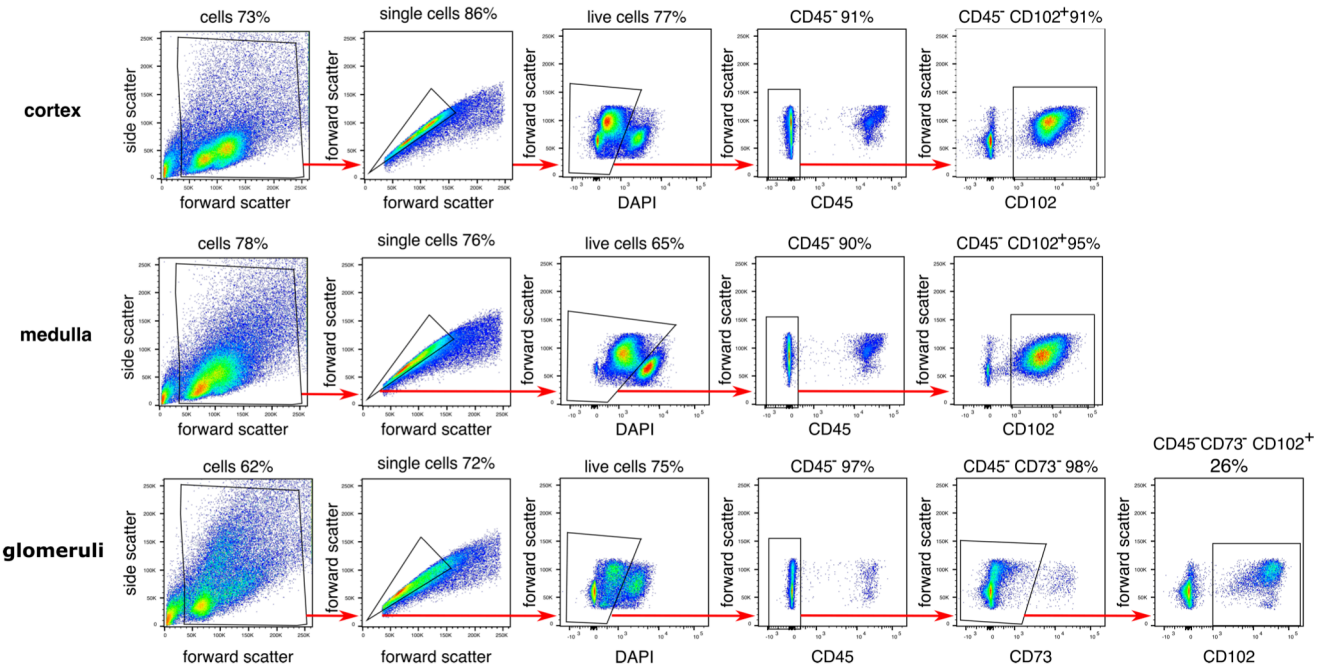

B *in silico* EC selection

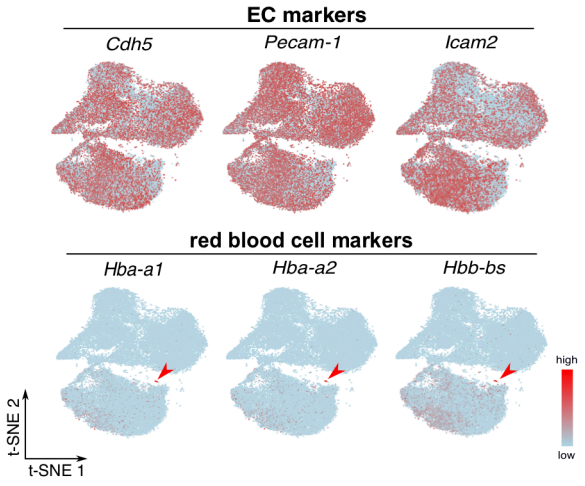

C metrics gRECs control

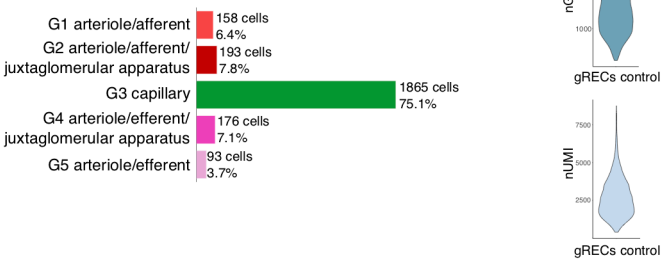

D metrics cRECs control

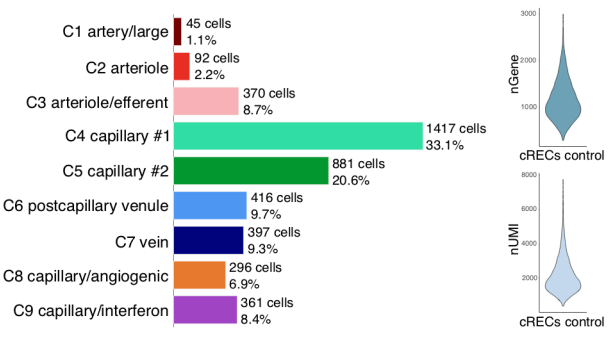

E metrics mRECs control

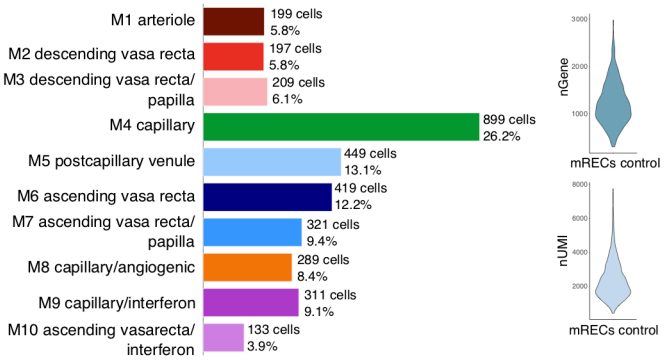

Figure S2

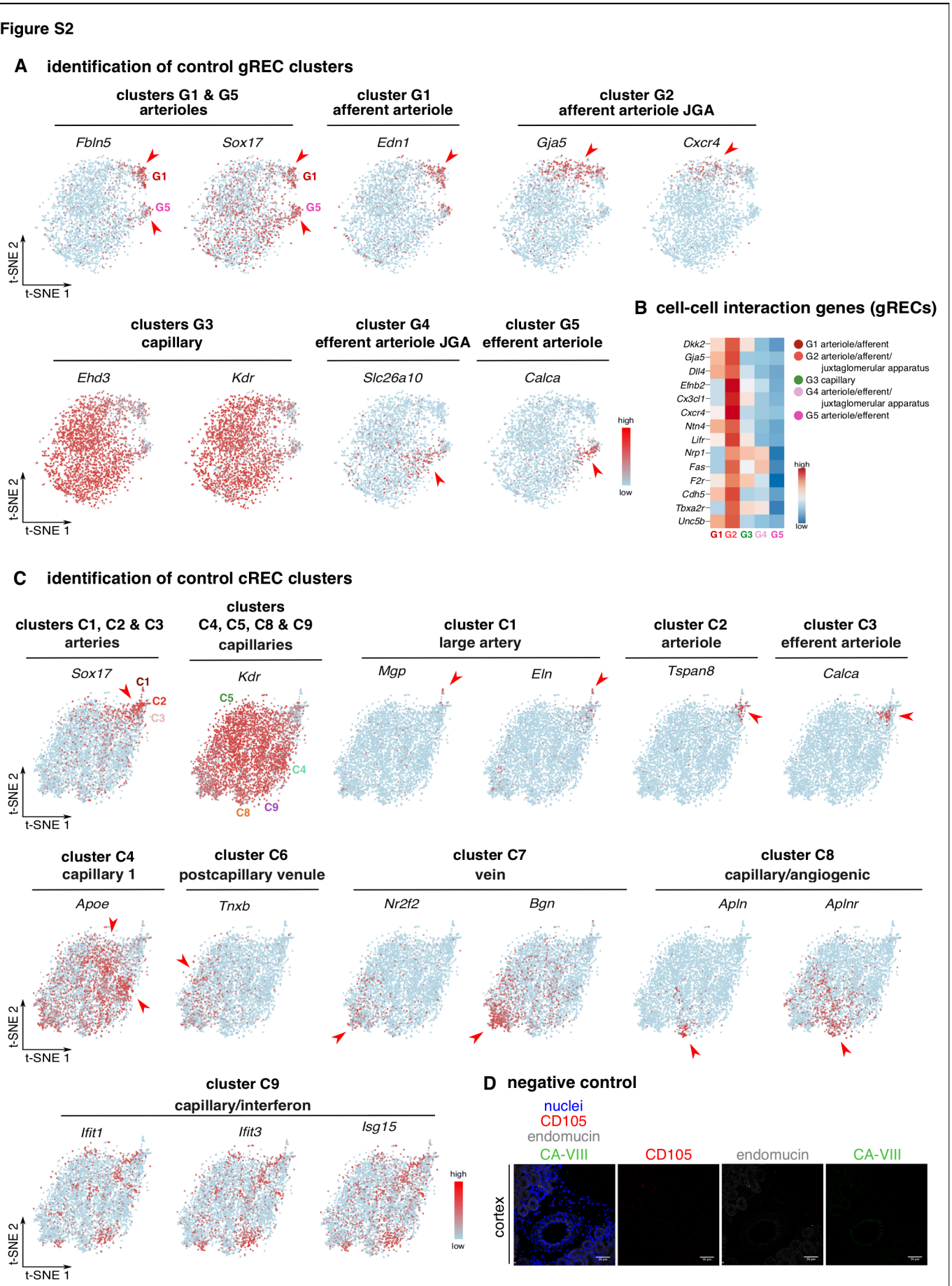
A identification of control gREC clusters
clusters G1 & G5 arterioles
cluster G1 afferent arteriole
cluster G2 afferent arteriole JGA
Fbln5
Sox17
Edn1
Gja5
Cxcr4
G1
G5
t-SNE 2
t-SNE 1
clusters G3 capillary
cluster G4 efferent arteriole JGA
cluster G5 efferent arteriole
Ehd3
Kdr
Slc26a10
Calca
high
low
B cell-cell interaction genes (gRECs)
Dkk2
Gja5
Dll4
Efnb2
Cx3cl1
Cxcr4
Ntn4
Lifr
Nrp1
Fas
F2r
Cdh5
Tbxa2r
Unc5b
G1 G2 G3 G4 G5
G1 arteriole/afferent
G2 arteriole/afferent/ juxtaglomerular apparatus
G3 capillary
G4 arteriole/efferent/ juxtaglomerular apparatus
G5 arteriole/efferent
C identification of control cREC clusters
clusters C1, C2 & C3 arteries
clusters C4, C5, C8 & C9 capillaries
cluster C1 large artery
cluster C2 arteriole
cluster C3 efferent arteriole
Sox17
Kdr
Mgp
Eln
Tspan8
Calca
C1
C2
C3
C4
C5
C8
C9
cluster C4 capillary 1
cluster C6 postcapillary venule
cluster C7 vein
cluster C8 capillary/angiogenic
Apoe
Tnxb
Nr2f2
Bgn
Apln
Aplnr
cluster C9 capillary/interferon
Ifit1
Ifit3
Isg15
D negative control
nuclei
CD105
endomucin
CA-VIII
cortex

Figure S3

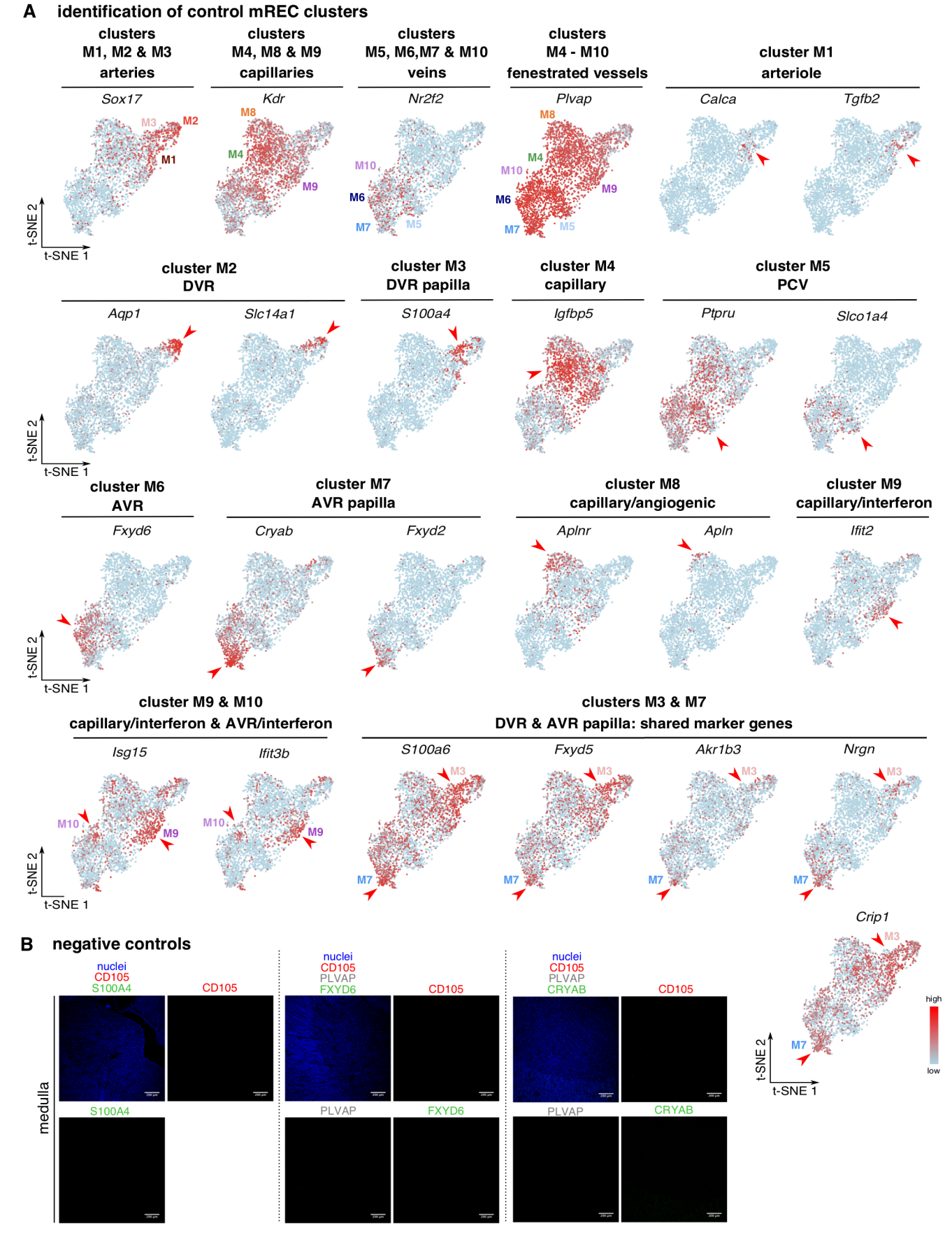
A identification of control mREC clusters
clusters M1, M2 & M3 arteries
clusters M4, M8 & M9 capillaries
clusters M5, M6,M7 & M10 veins
clusters M4 - M10 fenestrated vessels
cluster M1 arteriole
Sox17
Kdr
Nr2f2
Plvap
Calca
Tgfb2
cluster M2 DVR
cluster M3 DVR papilla
cluster M4 capillary
cluster M5 PCV
Aqp1
Slc14a1
S100a4
Igfbp5
Ptpru
Slco1a4
cluster M6 AVR
cluster M7 AVR papilla
cluster M8 capillary/angiogenic
cluster M9 capillary/interferon
Fxyd6
Cryab
Fxyd2
Aplnr
Apln
Ifit2
cluster M9 & M10 capillary/interferon & AVR/interferon
clusters M3 & M7 DVR & AVR papilla: shared marker genes
Isg15
Ifit3b
S100a6
Fxyd5
Akr1b3
Nrgn
Crip1
t-SNE 1
t-SNE 2
high
low
B negative controls
nuclei
CD105
S100A4
PLVAP
FXYD6
CRYAB
medulla

Figure S4

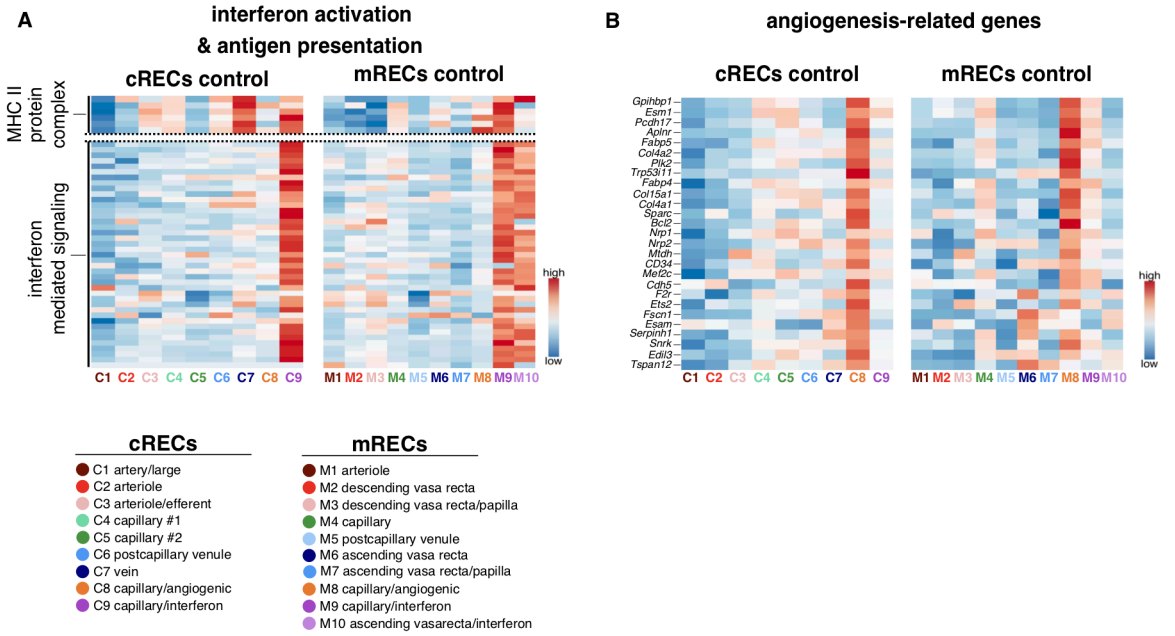
A
interferon activation
& antigen presentation
cRECs control
mRECs control
MHC II protein complex
interferon mediated signaling
high
low
C1 C2 C3 C4 C5 C6 C7 C8 C9
M1 M2 M3 M4 M5 M6 M7 M8 M9 M10
B
angiogenesis-related genes
cRECs control
mRECs control
Gpihbp1
Esm1
Pcdh17
Aplnr
Fabp5
Col4a2
Plk2
Trp53i11
Fabp4
Col15a1
Col4a1
Sparc
Bcl2
Nrp1
Nrp2
Mtdh
CD34
Mef2c
Cdh5
F2r
Ets2
Fscn1
Esam
Serpinh1
Snrk
Edil3
Tspan12
cRECs
C1 artery/large
C2 arteriole
C3 arteriole/efferent
C4 capillary #1
C5 capillary #2
C6 postcapillary venule
C7 vein
C8 capillary/angiogenic
C9 capillary/interferon
mRECs
M1 arteriole
M2 descending vasa recta
M3 descending vasa recta/papilla
M4 capillary
M5 postcapillary venule
M6 ascending vasa recta
M7 ascending vasa recta/papilla
M8 capillary/angiogenic
M9 capillary/interferon
M10 ascending vasarecta/interferon

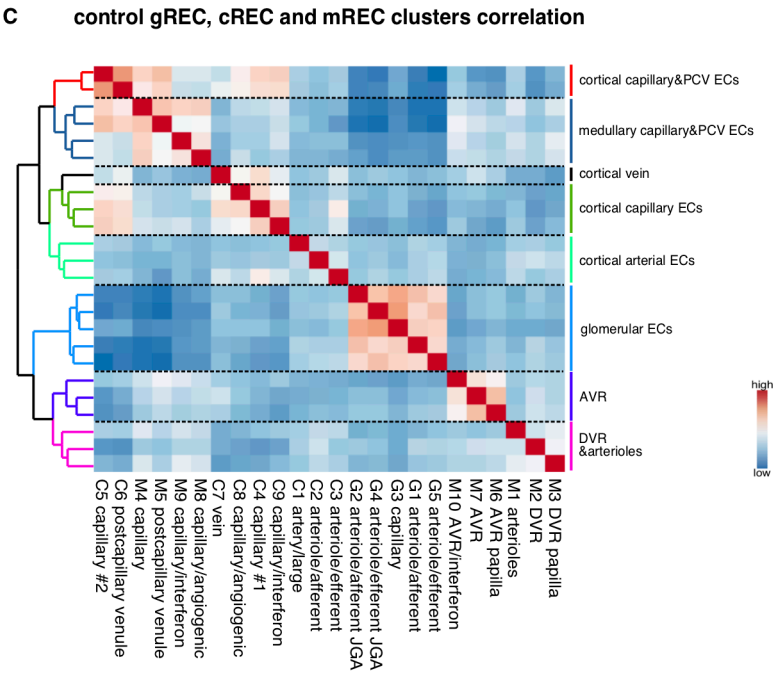
C
control gREC, cREC and mREC clusters correlation
cortical capillary&PCV ECs
medullary capillary&PCV ECs
cortical vein
cortical capillary ECs
cortical arterial ECs
glomerular ECs
AVR
DVR &arterioles
high
low
C5 capillary #2
C6 postcapillary venule
M4 capillary
M5 postcapillary venule
M9 capillary/interferon
M8 capillary/angiogenic
C7 vein
C8 capillary/angiogenic
C4 capillary #1
C9 capillary/interferon
C1 artery/large
C2 arteriole/afferent
C3 arteriole/efferent
G2 arteriole/efferent JGA
G4 arteriole/efferent JGA
G3 capillary
G1 arteriole/afferent
G5 arteriole/efferent
M10 AVR/interferon
M7 AVR
M6 AVR papilla
M1 arterioles
M2 DVR
M3 DVR papilla

Figure S5

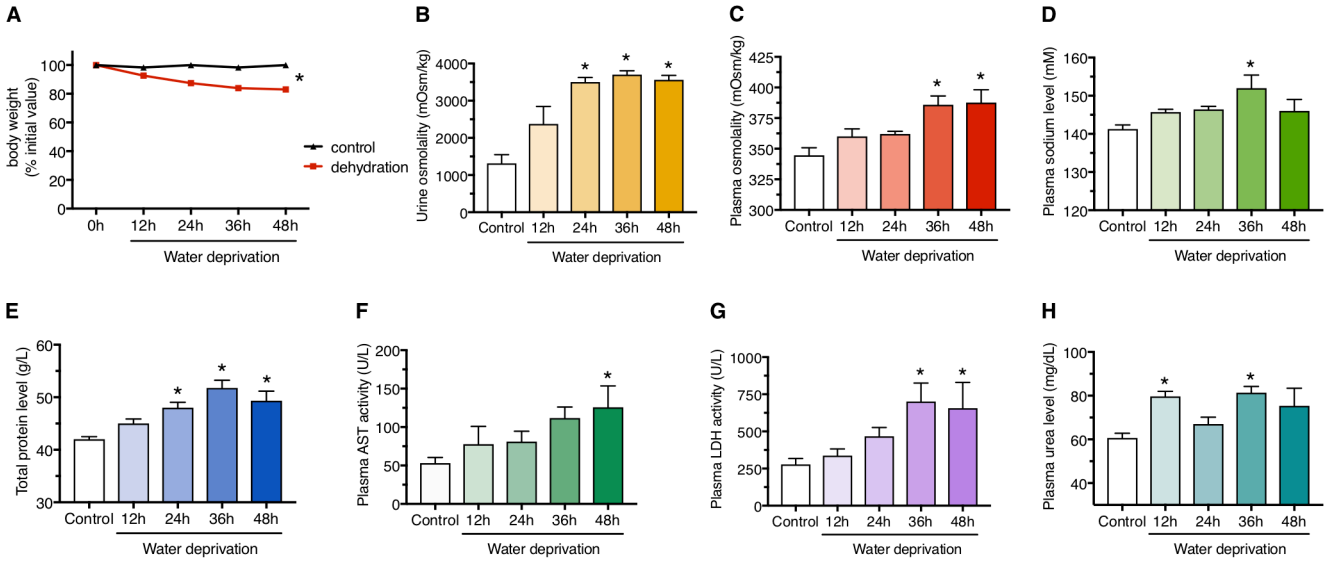
A
body weight (% initial value)
control
dehydration
0h 12h 24h 36h 48h
Water deprivation
B
Urine osmolality (mOsm/kg)
Control 12h 24h 36h 48h
Water deprivation
C
Plasma osmolality (mOsm/kg)
Control 12h 24h 36h 48h
Water deprivation
D
Plasma sodium level (mM)
Control 12h 24h 36h 48h
Water deprivation
E
Total protein level (g/L)
Control 12h 24h 36h 48h
Water deprivation
F
Plasma AST activity (U/L)
Control 12h 24h 36h 48h
Water deprivation
G
Plasma LDH activity (U/L)
Control 12h 24h 36h 48h
Water deprivation
H
Plasma urea level (mg/dL)
Control 12h 24h 36h 48h
Water deprivation

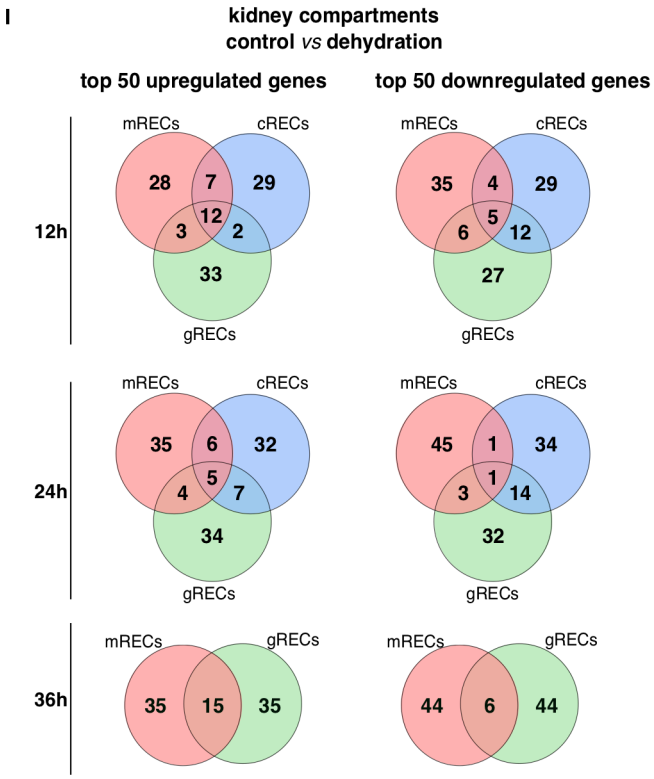
I
kidney compartments
control vs dehydration
top 50 upregulated genes
top 50 downregulated genes
12h
mRECs cRECs gRECs
28 7 29 12 3 2 33
35 4 29 5 6 12 27
24h
35 6 32 5 4 7 34
45 1 34 1 3 14 32
36h
mRECs gRECs
35 15 35
44 6 44

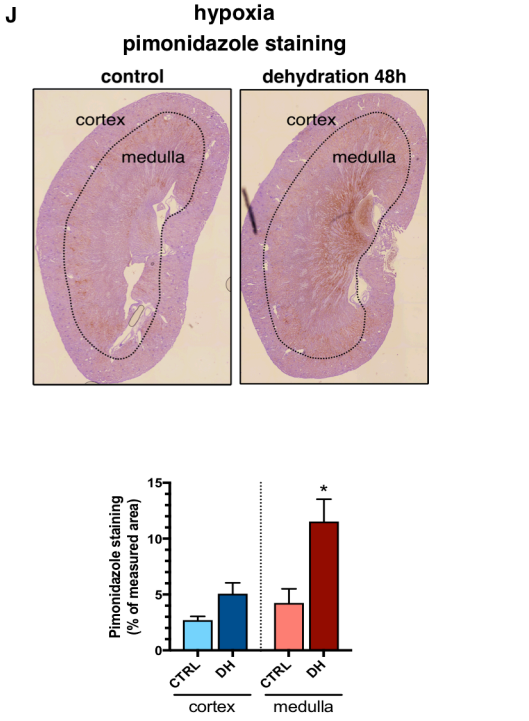
J
hypoxia
pimonidazole staining
control
dehydration 48h
cortex
medulla
Pimonidazole staining (% of measured area)
CTRL DH CTRL DH
cortex medulla

Figure S6

A

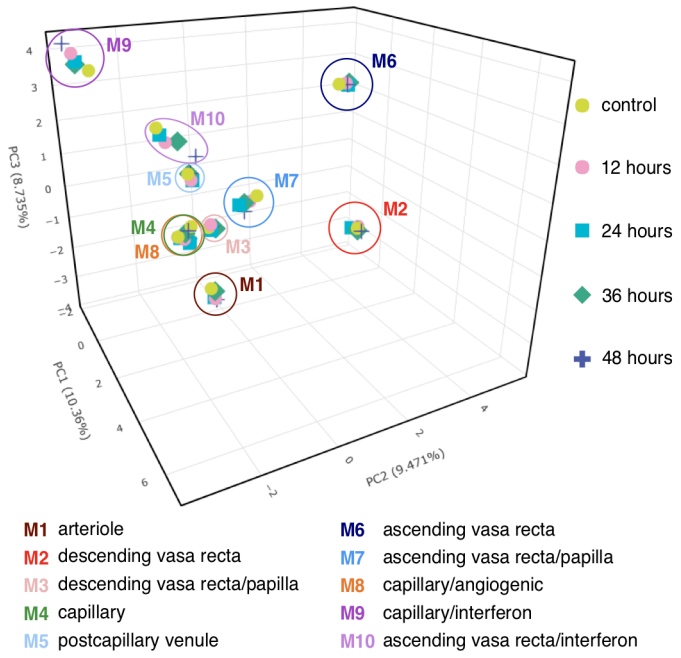

M1 arteriole
M2 descending vasa recta
M3 descending vasa recta/papilla
M4 capillary
M5 postcapillary venule
M6 ascending vasa recta
M7 ascending vasa recta/papilla
M8 capillary/angiogenic
M9 capillary/interferon
M10 ascending vasa recta/interferon

B **mREC cluster mapping similarity prediction control & dehydration**

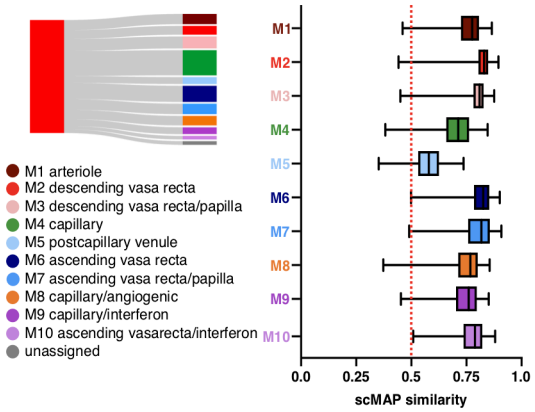

Figure S7

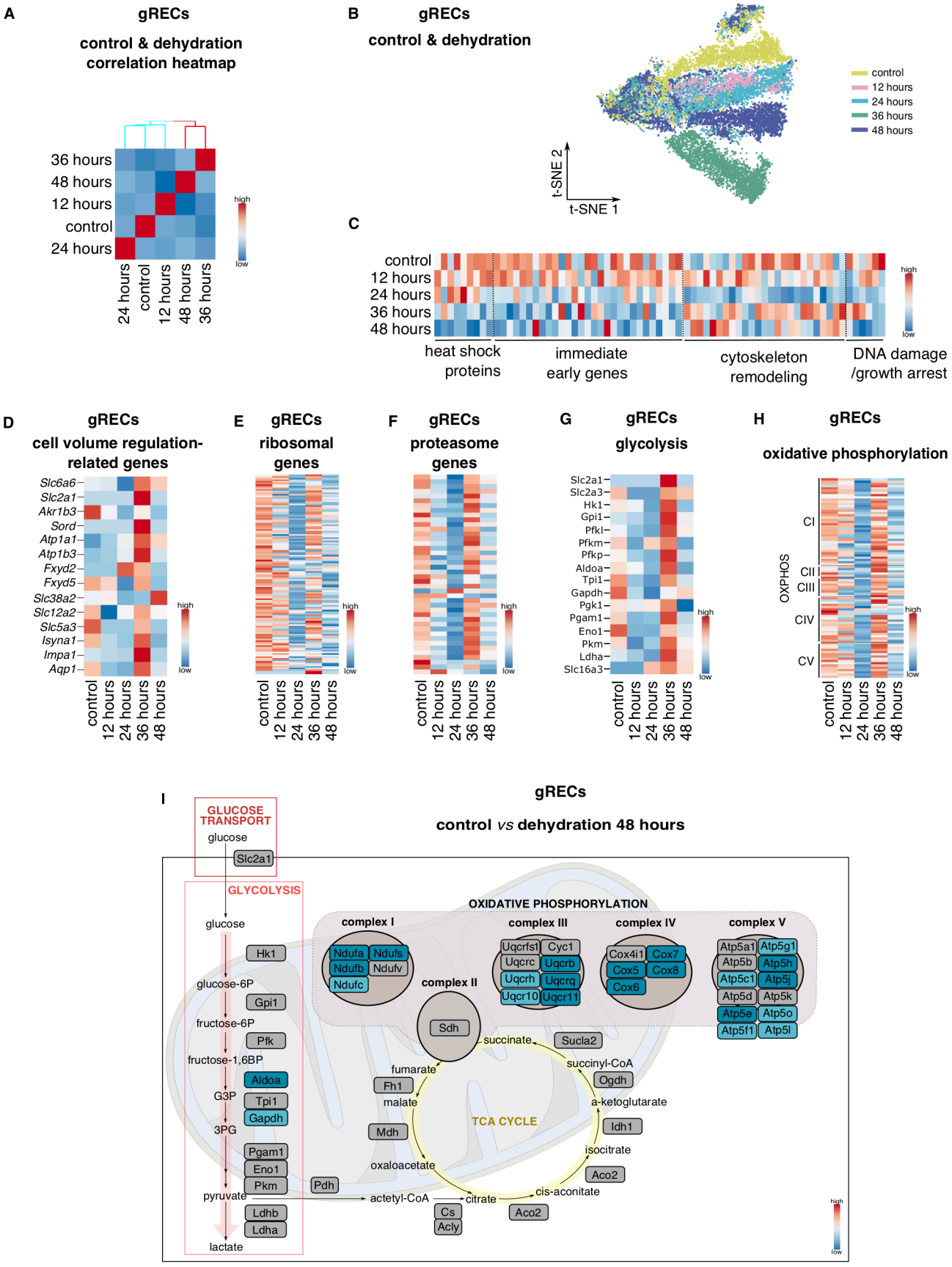
A
gRECs
control & dehydration
correlation heatmap
36 hours
48 hours
12 hours
control
24 hours
high
low
B
gRECs
control & dehydration
control
12 hours
24 hours
36 hours
48 hours
t-SNE 2
t-SNE 1
C
control
12 hours
24 hours
36 hours
48 hours
heat shock proteins
immediate early genes
cytoskeleton remodeling
DNA damage /growth arrest
D
gRECs
cell volume regulation-related genes
Slc6a6
Slc2a1
Akr1b3
Sord
Atp1a1
Atp1b3
Fxyd2
Fxyd5
Slc38a2
Slc12a2
Slc5a3
Isyna1
Impa1
Aqp1
E
gRECs
ribosomal genes
F
gRECs
proteasome genes
G
gRECs
glycolysis
Slc2a1
Slc2a3
Hk1
Gpi1
Pfkl
Pfkm
Pfkp
Aldoa
Tpi1
Gapdh
Pgk1
Pgam1
Eno1
Pkm
Ldha
Slc16a3
H
gRECs
oxidative phosphorylation
OXPHOS
CI
CII
CIII
CIV
CV
I
gRECs
control vs dehydration 48 hours
GLUCOSE TRANSPORT
glucose
Slc2a1
GLYCOLYSIS
glucose
Hk1
glucose-6P
Gpi1
fructose-6P
Pfk
fructose-1,6BP
Aldoa
G3P
Tpi1
Gapdh
3PG
Pgam1
Eno1
Pkm
pyruvate
Ldhb
Ldha
lactate
Pdh
OXIDATIVE PHOSPHORYLATION
complex I
Ndufa
Ndufs
Ndufb
Ndufv
Ndufc
complex II
Sdh
complex III
Uqcrfs1
Cyc1
Uqcrc
Uqcrb
Uqcrh
Uqcrq
Uqcr10
Uqcr11
complex IV
Cox4i1
Cox7
Cox5
Cox8
Cox6
complex V
Atp5a1
Atp5g1
Atp5b
Atp5h
Atp5c1
Atp5j
Atp5d
Atp5k
Atp5e
Atp5o
Atp5f1
Atp5l
succinate
Sucla2
succinyl-CoA
Ogdh
fumarate
Fh1
malate
a-ketoglutarate
TCA CYCLE
Idh1
Mdh
isocitrate
oxaloacetate
Aco2
cis-aconitate
actetyl-CoA
citrate
Cs
Acly
Aco2
high
low

Figure S8

A osmolyte content

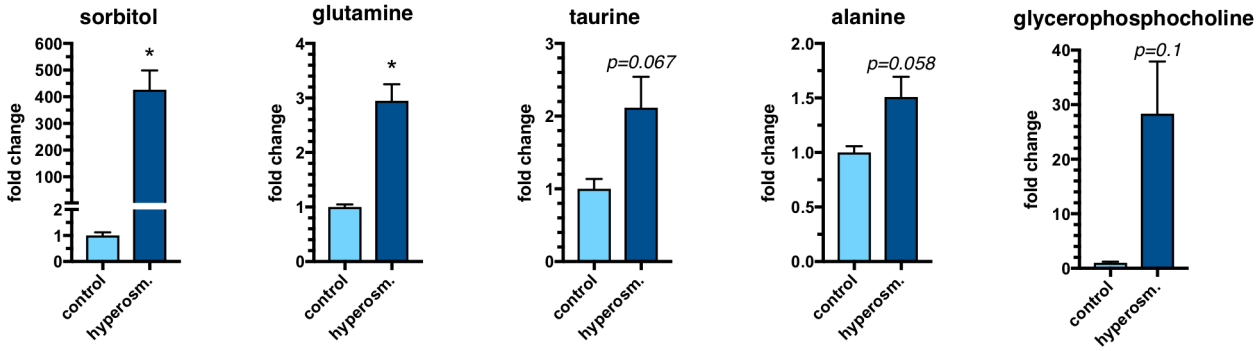

B Na^+/K^+ ATPase pump

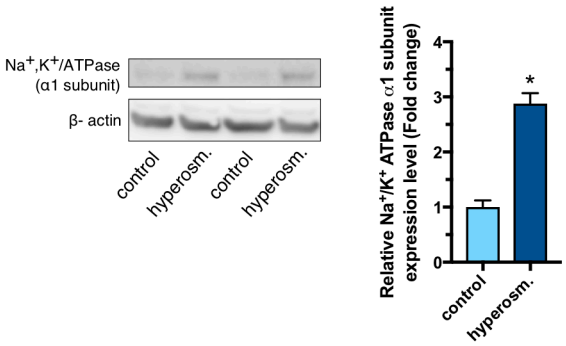

C basal respiration

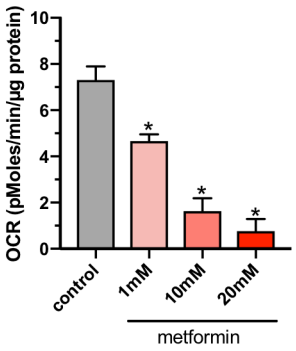

SUPPLEMENTARY FIGURE LEGENDS

Figure S1. EC SELECTION AND DATA METRICS FOR GRECS, CRECS AND MRECS (RELATED TO FIGURE 1, 2 AND 3)

(A) FACS strategy to sort RECs from kidney cortex, medulla and glomeruli. cRECs and mRECs were purified by FACS, sorting $CD45^{-}CD102^{+}$ cells, excluding $CD45^{+}$ leukocytes. gREC were isolated by FACS sorting $CD45^{-}CD73^{-}CD102^{+}$ cells, thereby excluding $CD45^{+}$ leukocytes and $CD73^{+}$ mesangial cells. (B) t-SNE plots of RECs from the three kidney compartments in control and dehydration conditions, color-coded for the expression of the indicated markers (*Pecam1*, *Cdh5* and *Icam2* for ECs; *Hbb-a1*, *Hbb-a2* and *Hbb-bs* for red blood cells that were excluded from downstream analyses). Red arrowheads indicate cells with high expression of the indicated marker on the t-SNE plot. Scale: light blue is low expression, red is high expression. (C-E) Bar graphs showing the number and percentage of analyzed RECs per cluster (left panel), and violin plots showing the number of genes and unique molecular identifiers (UMIs) (right panel) for gRECs (C), cRECs (D) and mRECs (E) in control conditions.

Figure S2. IDENTIFICATION OF GREC AND CREC SUBCLUSTERS (RELATED TO FIGURE 2)

(A) t-SNE plots of gRECs from the control condition, color-coded for the expression of the indicated markers. Red arrowheads indicate cells with high expression of the indicated marker on the t-SNE plot. Scale: light blue is low expression, red is high expression. (B) Expression level-scaled heatmap of cell-cell interaction-related genes in gRECs from the control condition. (C) t-SNE plots of cRECs from the control condition, color-coded for the expression of the indicated markers. Red arrowheads indicate cells with high expression of the indicated marker on the t-SNE plot. Scale: light blue is low expression, red is high expression. (D) Representative images of mouse kidney sections used as negative controls for the micrographs displayed in Figure 2H. Incubation with CD105 (red), endomucin (grey) and CA-VIII (green) was omitted. Nuclei are counterstained with Hoechst (blue). Scale bar, 200 µm.

Figure S3. IDENTIFICATION OF MREC SUBCLUSTERS (RELATED TO FIGURE 3)

(A) t-SNE plots of mRECs from the control condition, color-coded for the expression of the indicated markers. Red arrowheads indicate cells with high expression of the indicated marker on the t-SNE plot. Scale: light blue is low expression, red is high expression. (B) Representative images of mouse kidney sections used as negative controls for the micrographs displayed in Figures 3D-F. Incubation with CD105 (red), PLVAP (grey) and CRYAB (green) was omitted. Nuclei are counterstained with Hoechst (blue). Scale bar, 200 µm.

Figure S4. GREC, CREC AND MREC SUBCLUSTER ANALYSIS (RELATED TO FIGURES 2 AND 3)

(A,B) Expression level-scaled heatmap of interferon activated- and antigen presentation-related genes (A) and angiogenesis-related genes (B) in cRECs and mRECs from the control condition. Scale: light blue is low expression, red is high expression. (C) Correlation heatmap of all gREC, cREC and mREC subclusters. Scale: red indicates a high transcriptome similarity, blue indicates a low transcriptome similarity.

Figure S5. REC MOLECULAR ADAPTATION TO DEHYDRATION (RELATED TO FIGURE 4 AND 6)

(A) Body weight of mice subjected to control condition or water deprivation over time, expressed as percentage of initial body weight. (B-H) Urine osmolality (mOsm/kg) (B), plasma osmolality (mOsm/kg) (C), plasma sodium level (mM) (D), plasma total protein level (g/L) (E), plasma AST activity (U/L) (F), plasma LDH activity (U/L) (G), and plasma urea level (mg/dL) (H) of mice subjected to control condition or water deprivation over time. (I) Venn diagram of the top 50 up- (left) and downregulated (right) genes in RECs from the three kidney compartments at 12 hours of dehydration (top), 24 hours of dehydration (middle) and 36 hours of dehydration (bottom). Note for the 36 hours timepoint: the cREC sample did not meet sequencing quality standards and was therefore not included in downstream analyses. (J) (Top) Representative micrographs of kidney sections from mice subjected to control condition or 48

hours of water deprivation, stained for the hypoxia probe pimonidazole (brown). (Bottom) Pimonidazole staining quantification as expressed as percent of measured area for cortex and medulla from mice subjected to control condition or 48 hours of dehydration (DH). Data are mean ± SEM; n=3-6 mice/condition. Statistical tests: unpaired t-test, One- and Two-way ANOVA/Bonferroni, Kruskal-Wallis/Dunn's. *P<0.05.

Figure S6. RESPONSE OF MRECS SUBPOPULATIONS TO DEHYDRATION. (RELATED TO FIGURE 5)

(A) Principal component analysis plot of Jaccard similarity coefficient of mREC subpopulations in control and dehydrated mice. (B) scMap cluster projection of the control mREC phenotypes to all mRECs (i.e. including mRECs from the 12, 24, 36 and 48 hours of dehydration). Similarity scores of mRECs clusters are provided as boxplots. Unassigned cells are indicated in dark grey.

Figure S7. MOLECULAR AND METABOLIC ADAPTATION OF GRECS TO DEHYDRATION (RELATED TO FIGURE 5 AND 6)

(A) Correlation heatmap of gRECs from the control condition and at different dehydration time points. Scale: red indicates a high transcriptome similarity, blue indicates a low transcriptome similarity. (B) t-SNE plot color-coded for gRECs from the control condition and at different dehydration time points. (C-H) Expression level-scaled heatmaps of genes encoding heat shock proteins, or genes involved in cytoskeleton remodeling, DNA damage and growth arrest, and immediate early genes (C), cell volume regulation related genes (D), ribosome-related genes (E), proteasome-related genes (F), glycolysis-related genes (G) and oxidative phosphorylation-related genes (H), in gRECs from the control condition and at different dehydration time points. (I) Pathway map showing changes in transcript levels of metabolic genes from glycolysis, TCA cycle and OXPHOS in gRECs after 48 hours of dehydration compared with controls. Blue corresponds to low expression levels after dehydration; grey indicates that the change in gene expression did not reach the fold change threshold to be color-coded.

Figure S8. *IN VITRO* DEHYDRATION MODEL CHARACTERIZATION (RELATED TO FIGURE 7)

(A) Measurement of osmolyte content in control and hyperosmolarity (hyperosm)-exposed ECs: sorbitol, taurine, alanine, glutamine and glycerophosphocholine (n=3). (B) Left: Representative blot of Na^+/K^+ ATPase α1 subunit and β-actin in control and hyperosmolarity (hyperosm)-exposed ECs. Right: Densitometric quantification of the immunoblot signal of the Na^+/K^+ ATPase α1 subunit in control and hyperosmolarity (hyperosm)-exposed ECs (n=4). (C) Oxygen consumption rate (OCR) of control HUVECs pretreated with metformin (1 mM, 10 mM, 20 mM) or control vehicle for 1 hour. (n=3). Data are mean ± SEM. Statistical test: unpaired t-test, One-way ANOVA/Bonferroni. *P<0.05.

SUPPLEMENTAL METHODS

METABOLIC ASSAYS

Detection of organic osmolytes: Medium was removed and control HUVECs and hyperosmolarity-exposed HUVECs (900mOsm/kg) were washed with ice cold 0.9% NaCl. Osmolytes were extracted by adding 300 µL of a 80% methanol (in water) extraction buffer containing 2 µM of deuterated (d27) myristic acid (as internal standard) to the cells. Following extraction, precipitated proteins and insolubilities were removed by centrifugation at 20.000 x g for 15 min at 4°C. The supernatant was transferred to the appropriate mass spectrometer vials. Measurements were performed using a Dionex UltiMate 3000 LC System (Thermo Scientific) in-line connected to a Q-Exactive Orbitrap mass spectrometer (Thermo Scientific). 15 µl of sample was injected and loaded onto a Hilicon iHILIC-Fusion(P) column (Achrom). A linear gradient was carried out starting with 90% solvent A (LC-MS grade acetonitrile) and 10% solvent B (10 mM ammoniumacetate pH 9.3). From 2 to 20 minutes the gradient changed to 80% B and was kept at 80% until 23 min. Next a decrease to 40% B was carried out to 25 min, further decreasing to 10% B at 27 min. Finally, 10% B was maintained until 35 min. The solvent was used at a flow rate of 200 µl/min, the column temperature was kept constant at 25°C. The mass spectrometer operated in negative ion mode, settings of the HESI probe were as follows: sheath gas flow rate at 35, auxiliary gas flow rate at 10 (at a temperature of 260°C). Spray voltage was set at 4.8 kV, temperature of the capillary at 300°C and S-lens RF level at 50. A full scan (resolution of 140.000 and scan range of m/z 70-1050) was applied. For the data analysis we used an in-house library and sorbitol, glycerophosphocholine, taurine, alanine and glutamine were quantified (area under the curve) using the XCalibur 4.0 (Thermo Scientific) software platform. Measured values were normalized to protein content.

WESTERN BLOT

Protein lysates were separated by SDS-PAGE under reducing conditions, transferred to a nitrocellulose membrane, and analyzed by immunoblotting. Primary antibody used was rabbit anti-Na^+/K^+ ATPase α1 subunit (1/1000, 3010, Cell Signaling) and mouse anti-β actin (1/1000, A5441, Sigma) in 5% bovine serum albumin (BSA), appropriate secondary antibody was from Cell Signaling Technology (1:2000, Anti-Rabbit IgG HRP-linked #7074; 1:2000, Anti-Mouse IgG HRP-linked #7076) in 5% bovine serum albumin (BSA). Signal was detected using the ECL system (Pierce) according to the manufacturer's instructions. Densitometric quantifications of bands were done with Fiji software (https://fiji.sc).

HISTOLOGY AND IMMUNOHISTOCHEMISTRY

Renal Hypoxia: Renal hypoxia was detected after injection of 60 mg/kg pimonidazole hydrochloride (Hypoxyprobe kit, Chemicon-Millipore, Merck) into 48h-dehydrated and normally hydrated mice (kidneys were collected 2 hours after injection). To visualize the formation of pimonidazole adducts, kidney paraffin sections were immunostained with Hypoxyprobe-1-Mab1 following the manufacturer's instructions and counterstained with hematoxylin. Pimonidazole staining was quantified using Leica MetaMorph AF 2.1 morphometry software package (Leica).

SUPPLEMENTARY TABLES

Table S1. scRNA-seq data processing and visualization (Related to Figure 1-5, Figure S1-S3; S6)

Table S2. Top 50 marker genes for gRECs, cRECs and mRECs in control (Related to Figure 1)

Table S3. Molecular taxonomy of phenotypes of freshly isolated mouse RECs in control (Related to figure 2-3, Figure S2-S4)

Table S4. Top 50 marker genes for gREC, cREC and mRECs phenotypes in control (Related to Figure 2-3, Figure S2-S3)

Table S5. Geneset variation analysis of cREC and mREC phenotypes in control (Related to figure 2-3, Figure S2-S4)

Table S6. Differential analyses of cRECs, mRECs and gRECs in control vs different timepoints of dehydration (Related to Figure 4, Figure S5)

Table S7. Geneset enrichment analyses of mRECs in control vs 48 hour dehydration (Related to Figure 6)

Table S3: Molecular taxonomy of phenotypes of freshly isolated mouse RECs in control conditions. Related to Figures 2 and 3.

NOTE 1: Expression patterns of all genes in Tables S4, S5 and S6 (also of those not listed in the text, figures or Tables S4, S5 and S6) can be explored via the accompanying online web tool available from https://endotheliomics.shinyapps.io/rec_dehydration/ (**username**: RECdehydration@gmail.com; **password:** scRECpaper).

KIDNEY COMPARMENT	ASSIGNED PHENOTYPES	CLUS-TER NR	EXPRESSED GENES TYPICAL OF	FIG.	TABLE
GLOMERULI	afferent arteriole	G1	• arterial ECs (*Sox17, Sema3g, Gja4*) (Corada et al., 2013; Fang et al., 2017; Kutschera et al., 2011) • vascular integrity & elastic fiber assembly (*Ltbp4*, *Fbln5, Bmp4*) (Noda et al., 2013; Tojais et al., 2017) • tight junctions (*Cldn5*) (Morita et al., 1999) • Connexin 37 (*Gja4*), known to be present in gRECs from afferent arterioles but not efferent arterioles (Zhang and Hill, 2005) • vasotone regulation (*Edn1*, *Alox12, S1pr1*) (Cantalupo et al., 2017; Ma et al., 1991; Takeya et al., 2015; Yiu et al., 2003)	S2A S2A 2B, S2A	S4
	portion of the afferent arteriole associated with the juxtaglomerular apparatus	G2	• intermediate capillary-like and arterial-like EC phenotype (*Kdr, CD300lg, Efnb2, Dll4, Gja4, Gja5*) (Buschmann et al., 2010; Fang et al., 2017; Kamba et al., 2006; Rosivall and Peti-Peterdi, 2006; Shutter et al., 2000; Wang et al., 1998; Zhao et al., 2018) • gap junctions (*Gja5*), known to be present in gRECs from afferent arterioles but not efferent arterioles (Zhang and Hill, 2005), may contribute to the tubuloglomerular feedback in the juxtaglomerular apparatus (Just et al., 2009; Kurtz et al., 2010; Sorensen et al., 2012) • chemokine receptor, described to be expressed by RECs in contact with renin+ cells at this location (*Cxcr4*) (Takabatake et al., 2009) • cell-cell interaction (*Dkk2*, *Gja5*, *Dll4*, *Efnb2*, *Cx3cl1*, *Cxcr4*, *Ntn4*, *Lifr*, *Nrp1*, *Fas*, *F2r*, *Cdh5*, *Tbxa2r*, *Unc5b*) (Cunningham et al., 2000; Davis et al., 2019; Imaizumi et al., 2004; Just et al., 2009; Komhoff et al., 1998; Kurtz et al., 2010; Lejmi et al., 2008; Min et al., 2011; Sata et al., 2000; Shutter et al., 2000; Sorensen et al., 2012; Takabatake et al., 2009; Wang et al., 1998; Welti et al., 2013; Yamaguchi et al., 2012)	2B S2A, S2B S2A 2B, S2A, S2B 2B, S2B	
	capillary	G3	• capillary ECs (*Kdr*) (Kamba et al., 2006) • known glomerular capillary EC marker (*Ehd3*) (Patrakka et al., 2007) • Tgfβ/bmp signaling pathways (*Eng*, *Smad6*, *Smad7*, *Xiap*, *Hipk2*), involved in glomerular capillary formation (Cai et al., 2012; Liu et al., 1999; Shang et al., 2013; Ueda et al., 2008; Van Themsche et al., 2010)	2B, S2A 2B	
	portion of the efferent arteriole	G4	• intermediate capillary-like and arterial-like EC phenotype (*Kdr, Sox17*) (Corada et al., 2013; Kamba et al., 2006) • absence/low expression of connexins 37 and 40 (*Gja4*, *Gja5*) (Zhang and Hill, 2005)	S2A S2A	

	associated with the juxtaglomerular apparatus		• immune cell adhesion & extravasation, endothelial permeability (*CD9*, *Rdx*, *Gas6, Podxl, Sgk1, Pde2a, Clic1, Icam2, Endrb*) (Halai et al., 2014; Horrillo et al., 2016; Koehl et al., 2017; Koss et al., 2006; Ni et al., 2019; Reyes et al., 2018; Su et al., 2014; Surapisitchat et al., 2007; Xu et al., 2016)		
	efferent arteriole	G5	• arterial ECs (*Sox17)* (Corada et al., 2013) • absence/low expression of connexins 37 and 40 (*Gja4*, *Gja5*) (Zhang and Hill, 2005) • vasotone regulation (*Calca*) (Reslerova and Loutzenhiser, 1998) • prevention of coagulation (*Thbd*) (Isermann et al., 2001) • hyperosmolarity-responsive genes (*Klf4*, *S100a4*, *Slc6a6*, *Cryab*, *S100a6*, *Ptprr*, *CD200, Ebf1, Slc38a2*) (Alfieri et al., 2001; Izumi et al., 2015; Maallem et al., 2008; Schulze Blasum et al., 2016)	S2A S2A 2B, S2A 2B	
CORTEX	large artery	C1	• arterial ECs (*Sox17, Sema3g, Gja4, Gja5, Jag1*) (Buschmann et al., 2010; Corada et al., 2013; Fang et al., 2017; High et al., 2008; Kutschera et al., 2011) • suppression of calcification (*Mgp*) (Bjorklund et al., 2018) • tight junction (*Cldn5*) (Morita et al., 1999) • vascular integrity & elastic fiber assembly (*Eln, Ltbp4, Fbln5, Fbln2, Bmp4*) (Chapman et al., 2010; Noda et al., 2013; Tojais et al., 2017; Wagenseil and Mecham, 2012; Walker et al., 2015) • vasotone regulation (*Ace*, *Edn1*, *S1pr1*) (Arendshorst et al., 1990; Ma et al., 1991; Yiu et al., 2003) • response to shear stress (*Pi16*) (Hazell et al., 2016)	S2C 2E	S4
	arteriole	C2	• arteriolar ECs (*Sox17, Cxcl12*) (Corada et al., 2013; Poulos et al., 2018) • vasotone regulation (*Alox12*) (Cantalupo et al., 2017; Ma et al., 1991; Takeya et al., 2015; Yiu et al., 2003) • kidney function biomarker & angiostatic mediator (*Cst3*) (Benndorf, 2018; Li et al., 2018; Shlipak et al., 2013)	S2C	
	efferent arteriole	C3	• arteriolar ECs (*Sox17, Kitl*) (Corada et al., 2013; Poulos et al., 2018) • vasotone regulation (*Calca*) (Reslerova and Loutzenhiser, 1998) • prevention of coagulation (*Thbd*) (Isermann et al., 2001) • shared marker genes with cluster G5 (*Calca*, *Thbd*, *Rpl8*, *S100a6*, *CD200*, *Rplp0*, *Ifi27l2a*…)	S2C S2C 2E	
	capillary #1	C4	• fenestrated capillaries ECs (*Kdr, Plvap*) (Dimke et al., 2015; Stan et al., 1999) • lipid metabolism (*Plpp3, Apoe, Thrsp*) (Busnelli et al., 2018; Huang and Mahley, 2014; Yao et al., 2016) • microvascular remodeling (*Id3*) (Lee et al., 2014)	S2C 2E, S2C	
	capillary #2	C5	• fenestrated capillaries ECs (*Kdr, Plvap*) (Dimke et al., 2015; Stan et al., 1999) • VEGF receptors (*Kdr*, *Flt1, Nrp1*) (Welti et al., 2013) • Insulin-growth factor binding (*Igfbp5, Igfbp3, Insr*) (Pollak, 2012) • blood volume & sodium excretion regulation (*Npr3*) (Matsukawa et al., 1999; Potter, 2011)	2E, S2C 2E, S2C	
	postcapillary venule	C6	• intermediate fenestrated capillary-like and vein-like EC phenotype (*Kdr*, *Plvap*, *Nr2f2*) (Dimke et al., 2015; Stan et al., 1999; You et al., 2005) • regulation of endothelial permeability (*Jup*) (Nottebaum et al., 2008) • extracellular matrix (*Tnxb*, *Hspg2*, *Ltbp1*) (Gubbiotti et al., 2017; Ikuta et al., 2001; Robertson et al., 2015; Unsold et al., 2001; Valcourt et al., 2015)	S2C 2E	

			• vascular development/angiogenesis (*Pbx1*, *Arghap31*) (Caron et al., 2016; Charboneau et al., 2005)		
	vein	C7	• vein ECs (*Nr2f2*, *Plvap*) (Stan et al., 1999; You et al., 2005) • immune cell adhesion & extravasation, endothelial permeability (*Cd9, Gas6*) (Ni et al., 2019; Reyes et al., 2018)	S2C	
	capillary/angiogenic	C8	• fenestrated capillary ECs (*Kdr*, *Plvap*) (Dimke et al., 2015; Stan et al., 1999) • angiogenic EC markers (*Gpihbp1*, *Esm1*, *Col4a1*, *Col4a2*, *Trp53i11*, *Apln*, *Aplnr*, *Plk2*, *Fscn1*) (del Toro et al., 2010; Yang et al., 2015; Zhao et al., 2018)	S2C 2E, S2C, S4B	
	capillary/interferon	C9	• fenestrated capillary ECs (*Kdr*, *Plvap*) (Dimke et al., 2015; Stan et al., 1999) • interferon-stimulated genes (*Isg15*, *Ifit1*, *Ifit3*, *Ifi203*, *Ifit3b*, *Ifit2*, *Irf7*, *Ifi204*) (Schneider et al., 2014)	S2C 2E, S2C	
MEDULLA	arteriole	M1	• arteriolar ECs (*Sox17, Fbln5, Kitl*) (Corada et al., 2013; Poulos et al., 2018) • vascular integrity & elastic fiber assembly (*Ltbp4*) (Noda et al., 2013) • similar marker genes found in arterioles from cortex and glomeruli: G1, G5, C2 and C3 (*Thbd*, *Calca*, *Klf4*, *Tgfb2*, *Tm4sf1*, *Tsc22d1*, *Id1, Slc6a6, Cd24a, Kitl*) • shear stress (*Pi16*, *Klf2*, *Klf4*) (Clark et al., 2011; Hazell et al., 2016; Wang et al., 2010)	S3A 3B, S3A	S4
	descending vasa recta	M2	• arteriolar ECs (*Sox17*, *Gja4*, *Fbln5, Cxcl12*) (Corada et al., 2013; Poulos et al., 2018) • water and urea transport (*Aqp1*, *Slc14a1*) (Kim et al., 2002; Pallone et al., 2000) • vasotone regulation (*Hpgd*, *Edn1*, *Adipor2*) (Fesus et al., 2007; Silldorff et al., 1995) • tight junctions (*Cldn5*) (Morita et al., 1999)	S3A 3B, S3A	
	papillary portion of the descending vasa recta	M3	• arterial ECs (*Sox17, Fbln5*) (Corada et al., 2013) • vasotone regulation (*Alox12*) (Ma et al., 1991) • hyperosmolarity-responsive genes (*s100a4*, *s100a6*) (Nielsen et al., 1995; Schulze Blasum et al., 2016)	S3A 3B, S3A	
	capillary	M4	• fenestrated capillary ECs (*Kdr, Plvap*) (Dimke et al., 2015; Stan et al., 1999) • fatty acid transport and metabolism (*Cd36, Plpp3*) (Busnelli et al., 2018; Son et al., 2018) • VEGF receptors (*Kdr*, *Flt1, Nrp1*) (Welti et al., 2013) • blood volume & sodium excretion regulation (*Npr3*) (Matsukawa et al., 1999; Potter, 2011)	S3A S3A	
	postcapillary venule	M5	• intermediate fenestrated capillary-like and vein-like EC phenotype (*Kdr*, *Plvap*, *Nr2f2, Ephb4*) (Dimke et al., 2015; Stan et al., 1999; Wang et al., 1998; You et al., 2005) • regulation of endothelial permeability (*Jup*, *Bmpr2, Il6st*) (Alsaffar et al., 2018; Benn et al., 2016; Nottebaum et al., 2008)	S3A	
	ascending vasa recta	M6	• vein ECs (*Nr2f2*, *Plvap*) (Pannabecker and Dantzler, 2006; Stan et al., 1999; You et al., 2005) • angiopoietin receptor (*Tek*), necessary for ascending vasa recta development (Kenig-Kozlovsky et al., 2018) • immune cell adhesion & extravasation, endothelial permeability (*Gas6*) (Ni et al., 2019)	S3A	
	papillary portion of the ascending vasa recta	M7	• vein ECs (*Nr2f2*, *Plvap*) (Stan et al., 1999; You et al., 2005) • hyperosmolarity-responsive genes (*Cryab*, *Fxyd2*, *CD9*) (Izumi et al., 2015; Sheikh-Hamad et al., 1996) • anaerobic glycolysis (*Ldha*, *Aldoa*, *Gapdh*) (Chen et al., 2017; Eelen et al., 2015)	S3A 3B, S3A	
	capillary/angiogenic	M8	• fenestrated capillary ECs (*Kdr, Plvap*) (Dimke et al., 2015; Stan et al., 1999)	S3A	

			• angiogenic EC markers (*Gpihbp1*, *Col4a1*, *Col4a2*, *Trp53i11*, *Esm1*, *Aplnr*, *Plk2*) (del Toro et al., 2010; Yang et al., 2015; Zhao et al., 2018)	3B, S3A, S4B
	capillary/interferon	M9	• fenestrated capillary ECs (*Kdr*, *Plvap*) (Dimke et al., 2015; Stan et al., 1999) • interferon-stimulated genes (*Isg15*, *Ifi203*, *Ifit3b*, *Ifit2*, *Irf7*, *Ifitm3*, *Ifi204*) (Schneider et al., 2014)	S3A 3B, S3A
	ascending vasa recta/interferon	M10	• vein ECs (*Nr2f2*, *Plvap*) (Stan et al., 1999; You et al., 2005) • interferon-stimulated genes (*Ifit3*, *Ifit1*, *Ifi44*, *Iigp1*, *Irgm1*, *Ifi35*) (Schneider et al., 2014)	S3A S3A

References:

Alfieri, R.R., Petronini, P.G., Bonelli, M.A., Caccamo, A.E., Cavazzoni, A., Borghetti, A.F., and Wheeler, K.P. (2001). Osmotic regulation of ATA2 mRNA expression and amino acid transport System A activity. Biochem Biophys Res Commun *283*, 174-178.

Alsaffar, H., Martino, N., Garrett, J.P., and Adam, A.P. (2018). Interleukin-6 promotes a sustained loss of endothelial barrier function via Janus kinase-mediated STAT3 phosphorylation and de novo protein synthesis. Am J Physiol Cell Physiol *314*, C589-C602.

Arendshorst, W.J., Chatziantoniou, C., and Daniels, F.H. (1990). Role of angiotensin in the renal vasoconstriction observed during the development of genetic hypertension. Kidney Int Suppl *30*, S92-96.

Benn, A., Bredow, C., Casanova, I., Vukicevic, S., and Knaus, P. (2016). VE-cadherin facilitates BMP-induced endothelial cell permeability and signaling. J Cell Sci *129*, 206-218.

Benndorf, R.A. (2018). Renal Biomarker and Angiostatic Mediator? Cystatin C as a Negative Regulator of Vascular Endothelial Cell Homeostasis and Angiogenesis. J Am Heart Assoc *7*, e010997.

Bjorklund, G., Svanberg, E., Dadar, M., Card, D.J., Chirumbolo, S., Harrington, D.J., and Aaseth, J. (2018). The role of matrix Gla protein (MGP) in vascular calcification. Curr Med Chem.

Buschmann, I., Pries, A., Styp-Rekowska, B., Hillmeister, P., Loufrani, L., Henrion, D., Shi, Y., Duelsner, A., Hoefer, I., Gatzke, N., et al. (2010). Pulsatile shear and Gja5 modulate arterial identity and remodeling events during flow-driven arteriogenesis. Development *137*, 2187-2196.

Busnelli, M., Manzini, S., Parolini, C., Escalante-Alcalde, D., and Chiesa, G. (2018). Lipid phosphate phosphatase 3 in vascular pathophysiology. Atherosclerosis *271*, 156-165.

Cai, J., Pardali, E., Sanchez-Duffhues, G., and ten Dijke, P. (2012). BMP signaling in vascular diseases. FEBS Lett *586*, 1993-2002.

Cantalupo, A., Gargiulo, A., Dautaj, E., Liu, C., Zhang, Y., Hla, T., and Di Lorenzo, A. (2017). S1PR1 (Sphingosine-1-Phosphate Receptor 1) Signaling Regulates Blood Flow and Pressure. Hypertension *70*, 426-434.

Caron, C., DeGeer, J., Fournier, P., Duquette, P.M., Luangrath, V., Ishii, H., Karimzadeh, F., Lamarche-Vane, N., and Royal, I. (2016). CdGAP/ARHGAP31, a Cdc42/Rac1 GTPase regulator, is critical for vascular development and VEGF-mediated angiogenesis. Sci Rep *6*, 27485.

Chapman, S.L., Sicot, F.X., Davis, E.C., Huang, J., Sasaki, T., Chu, M.L., and Yanagisawa, H. (2010). Fibulin-2 and fibulin-5 cooperatively function to form the internal elastic lamina and protect from vascular injury. Arterioscler Thromb Vasc Biol *30*, 68-74.

Charboneau, A., East, L., Mulholland, N., Rohde, M., and Boudreau, N. (2005). Pbx1 is required for Hox D3-mediated angiogenesis. Angiogenesis *8*, 289-296.

Chen, Y., Fry, B.C., and Layton, A.T. (2017). Modeling glucose metabolism and lactate production in the kidney. Math Biosci *289*, 116-129.

Clark, P.R., Jensen, T.J., Kluger, M.S., Morelock, M., Hanidu, A., Qi, Z., Tatake, R.J., and Pober, J.S. (2011). MEK5 is activated by shear stress, activates ERK5 and induces KLF4 to modulate TNF responses in human dermal microvascular endothelial cells. Microcirculation *18*, 102-117.

Corada, M., Orsenigo, F., Morini, M.F., Pitulescu, M.E., Bhat, G., Nyqvist, D., Breviario, F., Conti, V., Briot, A., Iruela-Arispe, M.L., et al. (2013). Sox17 is indispensable for acquisition and maintenance of arterial identity. Nat Commun *4*, 2609.

Cunningham, M.A., Rondeau, E., Chen, X., Coughlin, S.R., Holdsworth, S.R., and Tipping, P.G. (2000). Protease-activated receptor 1 mediates thrombin-dependent, cell-mediated renal inflammation in crescentic glomerulonephritis. J Exp Med *191*, 455-462.

Davis, S.M., Collier, L.A., Goodwin, S., Lukins, D.E., Powell, D.K., and Pennypacker, K.R. (2019). Efficacy of leukemia inhibitory factor as a therapeutic for permanent large vessel stroke differs among aged male and female rats. Brain Res *1707*, 62-73.

del Toro, R., Prahst, C., Mathivet, T., Siegfried, G., Kaminker, J.S., Larrivee, B., Breant, C., Duarte, A., Takakura, N., Fukamizu, A., et al. (2010). Identification and functional analysis of endothelial tip cell-enriched genes. Blood *116*, 4025-4033.

Dimke, H., Sparks, M.A., Thomson, B.R., Frische, S., Coffman, T.M., and Quaggin, S.E. (2015). Tubulovascular cross-talk by vascular endothelial growth factor a maintains peritubular microvasculature in kidney. J Am Soc Nephrol *26*, 1027-1038.

Eelen, G., de Zeeuw, P., Simons, M., and Carmeliet, P. (2015). Endothelial cell metabolism in normal and diseased vasculature. Circ Res *116*, 1231-1244.

Fang, J.S., Coon, B.G., Gillis, N., Chen, Z., Qiu, J., Chittenden, T.W., Burt, J.M., Schwartz, M.A., and Hirschi, K.K. (2017). Shear-induced Notch-Cx37-p27 axis arrests endothelial cell cycle to enable arterial specification. Nat Commun *8*, 2149.

Fesus, G., Dubrovska, G., Gorzelniak, K., Kluge, R., Huang, Y., Luft, F.C., and Gollasch, M. (2007). Adiponectin is a novel humoral vasodilator. Cardiovasc Res *75*, 719-727.

Gubbiotti, M.A., Neill, T., and Iozzo, R.V. (2017). A current view of perlecan in physiology and pathology: A mosaic of functions. Matrix Biol *57-58*, 285-298.

Halai, K., Whiteford, J., Ma, B., Nourshargh, S., and Woodfin, A. (2014). ICAM-2 facilitates luminal interactions between neutrophils and endothelial cells in vivo. J Cell Sci *127*, 620-629.

Hazell, G.G., Peachey, A.M., Teasdale, J.E., Sala-Newby, G.B., Angelini, G.D., Newby, A.C., and White, S.J. (2016). PI16 is a shear stress and inflammation-regulated inhibitor of MMP2. Sci Rep *6*, 39553.

High, F.A., Lu, M.M., Pear, W.S., Loomes, K.M., Kaestner, K.H., and Epstein, J.A. (2008). Endothelial expression of the Notch ligand Jagged1 is required for vascular smooth muscle development. Proc Natl Acad Sci U S A *105*, 1955-1959.

Horrillo, A., Porras, G., Ayuso, M.S., and Gonzalez-Manchon, C. (2016). Loss of endothelial barrier integrity in mice with conditional ablation of podocalyxin (Podxl) in endothelial cells. Eur J Cell Biol *95*, 265-276.

Huang, Y., and Mahley, R.W. (2014). Apolipoprotein E: structure and function in lipid metabolism, neurobiology, and Alzheimer's diseases. Neurobiol Dis *72 Pt A*, 3-12.

Ikuta, T., Ariga, H., and Matsumoto, K.I. (2001). Effect of tenascin-X together with vascular endothelial growth factor A on cell proliferation in cultured embryonic hearts. Biol Pharm Bull *24*, 1320-1323.

Imaizumi, T., Yoshida, H., and Satoh, K. (2004). Regulation of CX3CL1/fractalkine expression in endothelial cells. J Atheroscler Thromb *11*, 15-21.

Isermann, B., Hendrickson, S.B., Zogg, M., Wing, M., Cummiskey, M., Kisanuki, Y.Y., Yanagisawa, M., and Weiler, H. (2001). Endothelium-specific loss of murine thrombomodulin disrupts the protein C anticoagulant pathway and causes juvenile-onset thrombosis. J Clin Invest *108*, 537-546.

Izumi, Y., Yang, W., Zhu, J., Burg, M.B., and Ferraris, J.D. (2015). RNA-Seq analysis of high NaCl-induced gene expression. Physiol Genomics *47*, 500-513.

Just, A., Kurtz, L., de Wit, C., Wagner, C., Kurtz, A., and Arendshorst, W.J. (2009). Connexin 40 mediates the tubuloglomerular feedback contribution to renal blood flow autoregulation. J Am Soc Nephrol *20*, 1577-1585.

Kamba, T., Tam, B.Y., Hashizume, H., Haskell, A., Sennino, B., Mancuso, M.R., Norberg, S.M., O'Brien, S.M., Davis, R.B., Gowen, L.C., et al. (2006). VEGF-dependent plasticity of fenestrated capillaries in the normal adult microvasculature. Am J Physiol Heart Circ Physiol *290*, H560-576.

Kenig-Kozlovsky, Y., Scott, R.P., Onay, T., Carota, I.A., Thomson, B.R., Gil, H.J., Ramirez, V., Yamaguchi, S., Tanna, C.E., Heinen, S., et al. (2018). Ascending Vasa Recta Are Angiopoietin/Tie2-Dependent Lymphatic-Like Vessels. J Am Soc Nephrol *29*, 1097-1107.

Kim, Y.H., Kim, D.U., Han, K.H., Jung, J.Y., Sands, J.M., Knepper, M.A., Madsen, K.M., and Kim, J. (2002). Expression of urea transporters in the developing rat kidney. Am J Physiol Renal Physiol *282*, F530-540.

Koehl, B., Nivoit, P., El Nemer, W., Lenoir, O., Hermand, P., Pereira, C., Brousse, V., Guyonnet, L., Ghinatti, G., Benkerrou, M., et al. (2017). The endothelin B receptor plays a crucial role in the adhesion of neutrophils to the endothelium in sickle cell disease. Haematologica *102*, 1161-1172.

Komhoff, M., Lesener, B., Nakao, K., Seyberth, H.W., and Nusing, R.M. (1998). Localization of the prostacyclin receptor in human kidney. Kidney Int *54*, 1899-1908.

Koss, M., Pfeiffer, G.R., 2nd, Wang, Y., Thomas, S.T., Yerukhimovich, M., Gaarde, W.A., Doerschuk, C.M., and Wang, Q. (2006). Ezrin/radixin/moesin proteins are phosphorylated by TNF-alpha and modulate permeability increases in human pulmonary microvascular endothelial cells. J Immunol *176*, 1218-1227.

Kurtz, L., Madsen, K., Kurt, B., Jensen, B.L., Walter, S., Banas, B., Wagner, C., and Kurtz, A. (2010). High-level connexin expression in the human juxtaglomerular apparatus. Nephron Physiol *116*, p1-8.

Kutschera, S., Weber, H., Weick, A., De Smet, F., Genove, G., Takemoto, M., Prahst, C., Riedel, M., Mikelis, C., Baulande, S., et al. (2011). Differential endothelial transcriptomics identifies semaphorin 3G as a vascular class 3 semaphorin. Arterioscler Thromb Vasc Biol *31*, 151-159.

Lee, D., Shenoy, S., Nigatu, Y., and Plotkin, M. (2014). Id proteins regulate capillary repair and perivascular cell proliferation following ischemia-reperfusion injury. PLoS One *9*, e88417.

Lejmi, E., Leconte, L., Pedron-Mazoyer, S., Ropert, S., Raoul, W., Lavalette, S., Bouras, I., Feron, J.G., Maitre-Boube, M., Assayag, F., et al. (2008). Netrin-4 inhibits angiogenesis via binding to neogenin and recruitment of Unc5B. Proc Natl Acad Sci U S A *105*, 12491-12496.

Li, Z., Wang, S., Huo, X., Yu, H., Lu, J., Zhang, S., Li, X., Cao, Q., Li, C., Guo, M., et al. (2018). Cystatin C Expression is Promoted by VEGFA Blocking, With Inhibitory Effects on Endothelial Cell Angiogenic Functions Including Proliferation, Migration, and Chorioallantoic Membrane Angiogenesis. J Am Heart Assoc *7*, e009167.

Liu, A., Dardik, A., and Ballermann, B.J. (1999). Neutralizing TGF-beta1 antibody infusion in neonatal rat delays in vivo glomerular capillary formation 1. Kidney Int *56*, 1334-1348.

Ma, Y.H., Harder, D.R., Clark, J.E., and Roman, R.J. (1991). Effects of 12-HETE on isolated dog renal arcuate arteries. Am J Physiol *261*, H451-456.

Maallem, S., Wierinckx, A., Lachuer, J., Kwon, M.H., and Tappaz, M.L. (2008). Gene expression profiling in brain following acute systemic hypertonicity: novel genes possibly involved in osmoadaptation. J Neurochem *105*, 1198-1211.

Matsukawa, N., Grzesik, W.J., Takahashi, N., Pandey, K.N., Pang, S., Yamauchi, M., and Smithies, O. (1999). The natriuretic peptide clearance receptor locally modulates the physiological effects of the natriuretic peptide system. Proc Natl Acad Sci U S A *96*, 7403-7408.

Min, J.K., Park, H., Choi, H.J., Kim, Y., Pyun, B.J., Agrawal, V., Song, B.W., Jeon, J., Maeng, Y.S., Rho, S.S., et al. (2011). The WNT antagonist Dickkopf2 promotes angiogenesis in rodent and human endothelial cells. J Clin Invest *121*, 1882-1893.

Morita, K., Sasaki, H., Furuse, M., and Tsukita, S. (1999). Endothelial claudin: claudin-5/TMVCF constitutes tight junction strands in endothelial cells. J Cell Biol *147*, 185-194.

Ni, J., Lin, M., Jin, Y., Li, J., Guo, Y., Zhou, J., Hong, G., Zhao, G., and Lu, Z. (2019). Gas6 Attenuates Sepsis-Induced Tight Junction Injury and Vascular Endothelial Hyperpermeability via the Axl/NF-κB Signaling Pathway. Frontiers in Pharmacology *10*.

Nielsen, S., Pallone, T., Smith, B.L., Christensen, E.I., Agre, P., and Maunsbach, A.B. (1995). Aquaporin-1 water channels in short and long loop descending thin limbs and in descending vasa recta in rat kidney. Am J Physiol *268*, F1023-1037.

Noda, K., Dabovic, B., Takagi, K., Inoue, T., Horiguchi, M., Hirai, M., Fujikawa, Y., Akama, T.O., Kusumoto, K., Zilberberg, L., et al. (2013). Latent TGF-beta binding protein 4 promotes elastic fiber assembly by interacting with fibulin-5. Proc Natl Acad Sci U S A *110*, 2852-2857.

Nottebaum, A.F., Cagna, G., Winderlich, M., Gamp, A.C., Linnepe, R., Polaschegg, C., Filippova, K., Lyck, R., Engelhardt, B., Kamenyeva, O., et al. (2008). VE-PTP maintains the endothelial barrier via plakoglobin and becomes dissociated from VE-cadherin by leukocytes and by VEGF. J Exp Med *205*, 2929-2945.

Pallone, T.L., Edwards, A., Ma, T., Silldorff, E.P., and Verkman, A.S. (2000). Requirement of aquaporin-1 for NaCl-driven water transport across descending vasa recta. J Clin Invest *105*, 215-222.

Pannabecker, T.L., and Dantzler, W.H. (2006). Three-dimensional architecture of inner medullary vasa recta. Am J Physiol Renal Physiol *290*, F1355-1366.

Patrakka, J., Xiao, Z., Nukui, M., Takemoto, M., He, L., Oddsson, A., Perisic, L., Kaukinen, A., Szigyarto, C.A., Uhlen, M., et al. (2007). Expression and subcellular distribution of novel glomerulus-associated proteins dendrin, ehd3, sh2d4a, plekhh2, and 2310066E14Rik. J Am Soc Nephrol *18*, 689-697.

Pollak, M. (2012). The insulin and insulin-like growth factor receptor family in neoplasia: an update. Nat Rev Cancer *12*, 159-169.

Potter, L.R. (2011). Natriuretic peptide metabolism, clearance and degradation. FEBS J *278*, 1808-1817.

Poulos, M., Redmond, D., Gutkin, M., Ramalingam, P., and Butler, J.M. (2018). Single-Cell Characterization of the HSC-Supportive Bone Marrow Vascular Microenvironment. Blood *132*, 2577-2577.

Reslerova, M., and Loutzenhiser, R. (1998). Renal microvascular actions of calcitonin gene-related peptide. Am J Physiol *274*, F1078-1085.

Reyes, R., Cardenes, B., Machado-Pineda, Y., and Cabanas, C. (2018). Tetraspanin CD9: A Key Regulator of Cell Adhesion in the Immune System. Front Immunol *9*, 863.

Robertson, I.B., Horiguchi, M., Zilberberg, L., Dabovic, B., Hadjiolova, K., and Rifkin, D.B. (2015). Latent TGF-beta-binding proteins. Matrix Biol *47*, 44-53.

Rosivall, L., and Peti-Peterdi, J. (2006). Heterogeneity of the afferent arteriole--correlations between morphology and function. Nephrol Dial Transplant *21*, 2703-2707.

Sata, M., Suhara, T., and Walsh, K. (2000). Vascular endothelial cells and smooth muscle cells differ in expression of Fas and Fas ligand and in sensitivity to Fas ligand-induced cell death: implications for vascular disease and therapy. Arterioscler Thromb Vasc Biol *20*, 309-316.

Schneider, W.M., Chevillotte, M.D., and Rice, C.M. (2014). Interferon-stimulated genes: a complex web of host defenses. Annu Rev Immunol *32*, 513-545.

Schulze Blasum, B., Schroter, R., Neugebauer, U., Hofschroer, V., Pavenstadt, H., Ciarimboli, G., Schlatter, E., and Edemir, B. (2016). The kidney-specific expression of genes can be modulated by the extracellular osmolality. FASEB J *30*, 3588-3597.

Shang, Y., Doan, C.N., Arnold, T.D., Lee, S., Tang, A.A., Reichardt, L.F., and Huang, E.J. (2013). Transcriptional corepressors HIPK1 and HIPK2 control angiogenesis via TGF-beta-TAK1-dependent mechanism. PLoS Biol *11*, e1001527.

Sheikh-Hamad, D., Ferraris, J.D., Dragolovich, J., Preuss, H.G., Burg, M.B., and Garcia-Perez, A. (1996). CD9 antigen mRNA is induced by hypertonicity in two renal epithelial cell lines. Am J Physiol *270*, C253-258.

Shlipak, M.G., Mattes, M.D., and Peralta, C.A. (2013). Update on cystatin C: incorporation into clinical practice. Am J Kidney Dis *62*, 595-603.

Shutter, J.R., Scully, S., Fan, W., Richards, W.G., Kitajewski, J., Deblandre, G.A., Kintner, C.R., and Stark, K.L. (2000). Dll4, a novel Notch ligand expressed in arterial endothelium. Genes Dev *14*, 1313-1318.

Silldorff, E.P., Yang, S., and Pallone, T.L. (1995). Prostaglandin E2 abrogates endothelin-induced vasoconstriction in renal outer medullary descending vasa recta of the rat. J Clin Invest *95*, 2734-2740.

Son, N.H., Basu, D., Samovski, D., Pietka, T.A., Peche, V.S., Willecke, F., Fang, X., Yu, S.Q., Scerbo, D., Chang, H.R., et al. (2018). Endothelial cell CD36 optimizes tissue fatty acid uptake. J Clin Invest *128*, 4329-4342.

Sorensen, C.M., Giese, I., Braunstein, T.H., Brasen, J.C., Salomonsson, M., and Holstein-Rathlou, N.H. (2012). Role of connexin40 in the autoregulatory response of the afferent arteriole. Am J Physiol Renal Physiol *303*, F855-863.

Stan, R.V., Kubitza, M., and Palade, G.E. (1999). PV-1 is a component of the fenestral and stomatal diaphragms in fenestrated endothelia. Proc Natl Acad Sci U S A *96*, 13203-13207.

Su, Y., Qadri, S.M., Cayabyab, F.S., Wu, L., and Liu, L. (2014). Regulation of methylglyoxal-elicited leukocyte recruitment by endothelial SGK1/GSK3 signaling. Biochim Biophys Acta *1843*, 2481-2491.

Surapisitchat, J., Jeon, K.I., Yan, C., and Beavo, J.A. (2007). Differential regulation of endothelial cell permeability by cGMP via phosphodiesterases 2 and 3. Circ Res *101*, 811-818.

Takabatake, Y., Sugiyama, T., Kohara, H., Matsusaka, T., Kurihara, H., Koni, P.A., Nagasawa, Y., Hamano, T., Matsui, I., Kawada, N., et al. (2009). The CXCL12 (SDF-1)/CXCR4 axis is essential for the development of renal vasculature. J Am Soc Nephrol *20*, 1714-1723.

Takeya, K., Wang, X., Kathol, I., Loutzenhiser, K., Loutzenhiser, R., and Walsh, M.P. (2015). Endothelin-1, but not angiotensin II, induces afferent arteriolar myosin diphosphorylation as a potential contributor to prolonged vasoconstriction. Kidney Int *87*, 370-381.

Tojais, N.F., Cao, A., Lai, Y.J., Wang, L., Chen, P.I., Alcazar, M.A.A., de Jesus Perez, V.A., Hopper, R.K., Rhodes, C.J., Bill, M.A., et al. (2017). Codependence of Bone Morphogenetic Protein Receptor 2 and Transforming Growth Factor-beta in Elastic Fiber Assembly and Its Perturbation in Pulmonary Arterial Hypertension. Arterioscler Thromb Vasc Biol *37*, 1559-1569.

Ueda, H., Miyazaki, Y., Matsusaka, T., Utsunomiya, Y., Kawamura, T., Hosoya, T., and Ichikawa, I. (2008). Bmp in podocytes is essential for normal glomerular capillary formation. J Am Soc Nephrol *19*, 685-694.

Unsold, C., Hyytiainen, M., Bruckner-Tuderman, L., and Keski-Oja, J. (2001). Latent TGF-beta binding protein LTBP-1 contains three potential extracellular matrix interacting domains. J Cell Sci *114*, 187-197.

Valcourt, U., Alcaraz, L.B., Exposito, J.Y., Lethias, C., and Bartholin, L. (2015). Tenascin-X: beyond the architectural function. Cell Adh Migr *9*, 154-165.

Van Themsche, C., Chaudhry, P., Leblanc, V., Parent, S., and Asselin, E. (2010). XIAP gene expression and function is regulated by autocrine and paracrine TGF-beta signaling. Mol Cancer *9*, 216.

Wagenseil, J.E., and Mecham, R.P. (2012). Elastin in large artery stiffness and hypertension. J Cardiovasc Transl Res *5*, 264-273.

Walker, A.E., Henson, G.D., Reihl, K.D., Morgan, R.G., Dobson, P.S., Nielson, E.I., Ling, J., Mecham, R.P., Li, D.Y., Lesniewski, L.A., et al. (2015). Greater impairments in cerebral artery compared with skeletal muscle feed artery endothelial function in a mouse model of increased large artery stiffness. J Physiol *593*, 1931-1943.

Wang, H.U., Chen, Z.F., and Anderson, D.J. (1998). Molecular distinction and angiogenic interaction between embryonic arteries and veins revealed by ephrin-B2 and its receptor Eph-B4. Cell *93*, 741-753.

Wang, W., Ha, C.H., Jhun, B.S., Wong, C., Jain, M.K., and Jin, Z.G. (2010). Fluid shear stress stimulates phosphorylation-dependent nuclear export of HDAC5 and mediates expression of KLF2 and eNOS. Blood *115*, 2971-2979.

Welti, J., Loges, S., Dimmeler, S., and Carmeliet, P. (2013). Recent molecular discoveries in angiogenesis and antiangiogenic therapies in cancer. J Clin Invest *123*, 3190-3200.

Xu, Y., Zhu, J., Hu, X., Wang, C., Lu, D., Gong, C., Yang, J., and Zong, L. (2016). CLIC1 Inhibition Attenuates Vascular Inflammation, Oxidative Stress, and Endothelial Injury. PLoS One *11*, e0166790.

Yamaguchi, I., Tchao, B.N., Burger, M.L., Yamada, M., Hyodo, T., Giampietro, C., and Eddy, A.A. (2012). Vascular endothelial cadherin modulates renal interstitial fibrosis. Nephron Exp Nephrol *120*, e20-31.

Yang, H., Fang, L., Zhan, R., Hegarty, J.M., Ren, J., Hsiai, T.K., Gleeson, J.G., Miller, Y.I., Trejo, J., and Chi, N.C. (2015). Polo-like kinase 2 regulates angiogenic sprouting and blood vessel development. Dev Biol *404*, 49-60.

Yao, D.W., Luo, J., He, Q.Y., Wu, M., Shi, H.B., Wang, H., Wang, M., Xu, H.F., and Loor, J.J. (2016). Thyroid hormone responsive (THRSP) promotes the synthesis of medium-chain fatty acids in goat mammary epithelial cells. J Dairy Sci *99*, 3124-3133.

Yiu, S.S., Zhao, X., Inscho, E.W., and Imig, J.D. (2003). 12-Hydroxyeicosatetraenoic acid participates in angiotensin II afferent arteriolar vasoconstriction by activating L-type calcium channels. J Lipid Res *44*, 2391-2399.

You, L.R., Lin, F.J., Lee, C.T., DeMayo, F.J., Tsai, M.J., and Tsai, S.Y. (2005). Suppression of Notch signalling by the COUP-TFII transcription factor regulates vein identity. Nature *435*, 98-104.

Zhang, J., and Hill, C.E. (2005). Differential connexin expression in preglomerular and postglomerular vasculature: accentuation during diabetes. Kidney Int *68*, 1171-1185.

Zhao, Q., Eichten, A., Parveen, A., Adler, C., Huang, Y., Wang, W., Ding, Y., Adler, A., Nevins, T., Ni, M., et al. (2018). Single-Cell Transcriptome Analyses Reveal Endothelial Cell Heterogeneity in Tumors and Changes following Antiangiogenic Treatment. Cancer Res *78*, 2370-2382.